

Comparison of ELM Pulse Propagation in the DIII-D SOL and Divertors with an Ion Convection Model

M. E. Fenstermacher, G. D. Porter, A. W. Leonard, N. H. Brooks, J. A. Boedo, R. J. Colchin, D. S. Gray, R. J. Groebner, M. Groth, J. T. Hogan, E. Hollmann, C. J. Lasnier, T. H. Osborne, T. W. Petrie, D. L. Rudakov, P. B. Snyder, H. Takahashi, J. G. Watkins, L. Zeng

U.S. Department of Energy

Lawrence
Livermore
National
Laboratory

This article was submitted to: *30th EPS Conference on Controlled Fusion and Plasma Physics, St Petersburg, Russia*
7/07/2003 – 7/11/2003

June 23, 2003

DISCLAIMER

This document was prepared as an account of work sponsored by an agency of the United States Government. Neither the United States Government nor the University of California nor any of their employees, makes any warranty, express or implied, or assumes any legal liability or responsibility for the accuracy, completeness, or usefulness of any information, apparatus, product, or process disclosed, or represents that its use would not infringe privately owned rights. Reference herein to any specific commercial product, process, or service by trade name, trademark, manufacturer, or otherwise, does not necessarily constitute or imply its endorsement, recommendation, or favoring by the United States Government or the University of California. The views and opinions of authors expressed herein do not necessarily state or reflect those of the United States Government or the University of California, and shall not be used for advertising or product endorsement purposes.

This is a preprint of a paper intended for publication in a journal or proceedings. Since changes may be made before publication, this preprint is made available with the understanding that it will not be cited or reproduced without the permission of the author.

This work was performed under the auspices of the United States Department of Energy by the University of California, Lawrence Livermore National Laboratory under contract No. W-7405-Eng-48.

This report has been reproduced directly from the best available copy.

Available electronically at <http://www.doc.gov/bridge>

Available for a processing fee to U.S. Department of Energy
And its contractors in paper from
U.S. Department of Energy
Office of Scientific and Technical Information
P.O. Box 62
Oak Ridge, TN 37831-0062
Telephone: (865) 576-8401
Facsimile: (865) 576-5728
E-mail: reports@adonis.osti.gov

Available for the sale to the public from
U.S. Department of Commerce
National Technical Information Service
5285 Port Royal Road
Springfield, VA 22161
Telephone: (800) 553-6847
Facsimile: (703) 605-6900
E-mail: orders@ntis.fedworld.gov
Online ordering: <http://www.ntis.gov/ordering.htm>

OR

Lawrence Livermore National Laboratory
Technical Information Department's Digital Library
<http://www.llnl.gov/tid/Library.html>

Comparison of ELM Pulse Propagation in the DIII-D SOL and Divertors with an Ion Convection Model

M.E. Fenstermacher,¹ G.D. Porter,¹ A.W. Leonard,² N.H. Brooks,² J.A. Boedo,³
R.J. Colchin,⁴ D.S. Gray,³ R.J. Groebner,² M. Groth,¹ J.T. Hogan,⁴ E. Hollmann,³
C.J. Lasnier,¹ T.H. Osborne,² T.W. Petrie,² D.L. Rudakov,³ P.B. Snyder,² H. Takahashi,⁵
J.G. Watkins,⁶ L. Zeng,⁷ and the DIII-D Team

DIII-D National Fusion Facility, San Diego, California, 92186-5608, USA

¹*Lawrence Livermore National Laboratory, Livermore, California, USA*

²*General Atomics, P.O. Box 85608, San Diego, California, USA*

³*University of California San Diego, San Diego, California, USA*

⁴*Oak Ridge National Laboratory, Oak Ridge, Tennessee, USA*

⁵*Princeton Plasma Physics Laboratory, Princeton, New Jersey, USA*

⁶*Sandia National Laboratory, Albuquerque, New Mexico, USA*

⁷*University of California Los Angeles, Los Angeles, California, USA*

Abstract. Results from dedicated ELM experiments, performed in DIII-D with fast diagnostics to measure the evolution of Type-I ELM effects in the SOL and divertor, are compared with a simple ion convection model and with initial time-dependent UEDGE simulations. Delays between ELM effects observed in the inner versus the outer divertor regions in the experiments scale, as a function of density, with the difference in ion convection time along field lines from the outer midplane to the divertor targets. The ELM perturbation was modeled as an instantaneous radially uniform increase of diffusion coefficients from the top of the pedestal to the outer SOL. The perturbation was confined to a poloidal zone approximately +70 and -90 cm from the outer midplane. The delays in the simulations are similar to these observed in the experiments.

1. Summary of Experimental Results

In experiments designed to characterize the effects of Type-I ELMs on the SOL and divertor [1-4] one observation was that for plasmas with line averaged density in the range $0.4 < n_e/n_{Gr} < 0.8$ (where n_{Gr} is the Greenwald density), the perturbation of D_α emission in the inner divertor was delayed from that in the outer divertor (Fig. 1). As the density and temperature of the pedestal and SOL plasma were varied by gas puffing the delay scaled with the difference in ion transit time, from the outer midplane to the two targets, $t_{transit} = \Delta L_c / C_s (T_e^{r_{\sim}})$ where $\Delta L_c = L_c^{in} - L_c^{out}$, $L_c^{in(out)}$, are the connection lengths between the outer midplane and the ISP (OSP) along the SOL field line connecting the locations of the D_α view spots on the targets, and $C_s (T_e^{r_{\sim}})$ is the ion sound

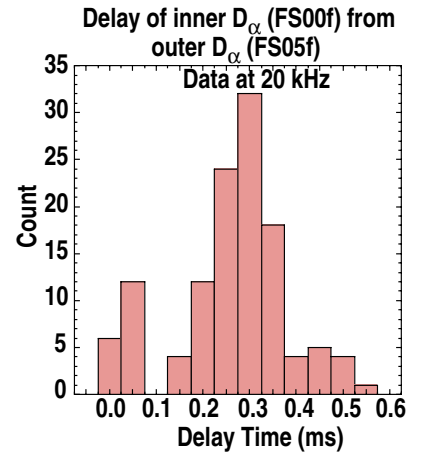


Fig. 1. Histogram of delay times of inner target D_α emission response to ELMs from outer divertor ELM response on the SOL flux surface that maps to ~ 3.5 cm from the midplane separatrix.

speed evaluated at the pedestal electron temperature before the ELM onset (Fig. 2). This observation and several others [1] were consistent with a simple model of ELM propagation in the SOL in which the time scale of particle and energy perturbation at the divertor targets is set by parallel propagation along SOL field lines at the ion sound speed of pedestal ejected particles [5]. It was observed [1] that the magnetics activity, and the D_α increase at the outer midplane and at the divertors, occurred several hundred microseconds prior to the drop of the pedestal ECE and soft x-ray (pedestal thermal energy loss) (Fig. 3). Also responding to the ELM instability prior to the thermal energy loss were the line-integrated density along a vertical chord in the outer divertor leg, the target ion saturation current and tile temperature, and the current integrated on target tiles (Fig. 3).

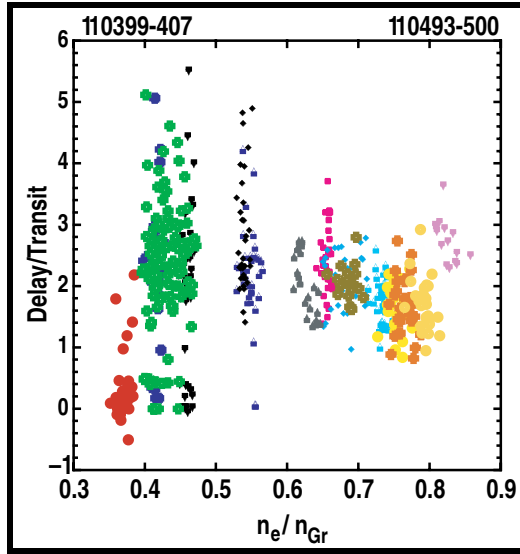


Fig. 2. Delay of inner target D_α emission response to ELMs from time of outer divertor ELM response normalized to difference in ion transit time as a function of normalized line averaged density.

2. UEDGE Simulations

The UEDGE multi-species fluid code [6] was used in time-dependent mode, with an increase in transport coefficients for a short period, to simulate the ELM perturbation of the pedestal and SOL. The initial steady-state H-mode solution prior to the ELM perturbation (Fig. 4) included a fluid neutrals model, all six charges species of carbon in a fluid impurities model and particle drift effects [7]. Neutrals in the model are assumed to be equilibrated by

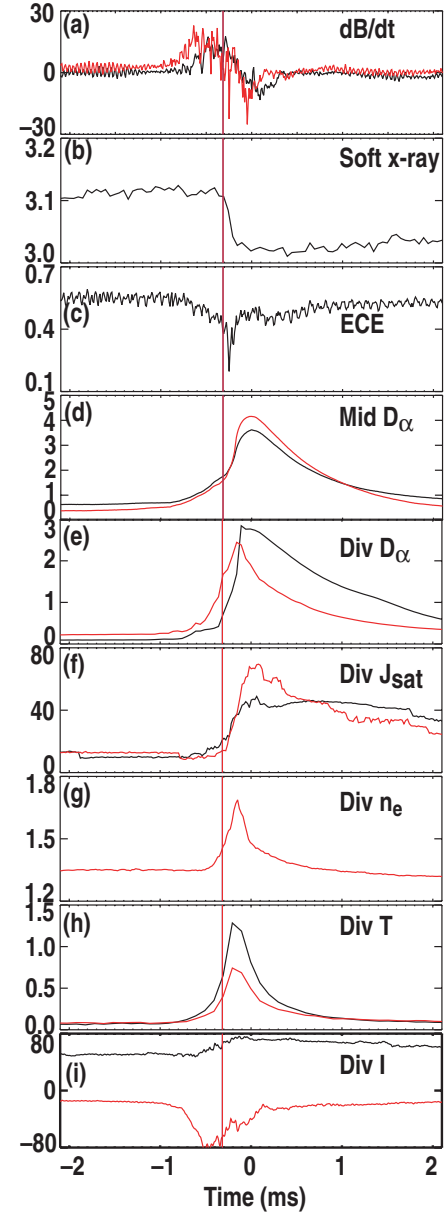


Fig. 3. Time evolution of average-ELM response of (a) dB/dt (T/s), (b) soft-x-ray signal, (c) ECE signal, (d) midplane D_α , and in the divertor (e) D_α , (f) J_{sat} , (g) line integrated n_e , (h) target temperature, (i) target tile current for inner(black) and outer (red) divertor channels.

charge-exchange with the local ion temperature and carbon sources from physical and chemical sputtering are calculated from the Haasz model [8]. The drift effects include ion $B \times \nabla B$ and $E \times B$ drifts but in these initial simulations the magnitude of the drifts was set to 20% of the full value predicted by theory. Work attempting to get converged solutions for stronger drifts, approaching the theoretical values, is in progress. As suggested by experimental observations, the ELM perturbation was modeled by an instantaneous $2.5\times$ increase in the particle diffusion coefficient for $550\ \mu\text{s}$. For the last $50\ \mu\text{s}$ of this period the energy transport coefficients were also increased by 25% over the steady state values. The perturbation was applied uniformly across the entire radius from the top of the pedestal to the outer SOL, but only within a poloidal zone of $+67.5$ to -93.0 cm from the outer midplane.

The steady-state UEDGE solution including full carbon species and reduced drift effects was well matched to experimental measurements between ELMs (Fig 4). The ion density and the power at the inner most grid surface were set to the experimental values. The power crossing the separatrix and the profiles of n_e and T_e in the SOL and pedestal gradient region at the outer midplane matched the measurements well [Fig. 4(a,b)]. The calculated carbon density (and n_e) at the top of the pedestal was comparable to that measured by CER [Fig. 4(c)]. Finally, the calculated profiles of line integrated D_α and CIII emission agreed with measurements in the divertor region at the chord locations although fine spatial structure was evident in the simulated profiles that can not be resolved by the finite measurements.

Initial simulations with the ELM perturbation show delays in D_α response in the inner divertor vs. the outer divertor that are similar to those measured although other details of the calculated evolution do not match measurements (Fig. 5). Simulations were run for a single ELM with a maximum time step of $25\ \mu\text{s}$ to focus on propagation of the perturbation in the SOL with temporal resolution similar to the D_α measurement. Runs with multiple ELMs were also done using variable time steps to examine the recovery phase after the transport coefficients were set back to the pre-ELM values. The recovery of the solution after the first ELM perturbation is not

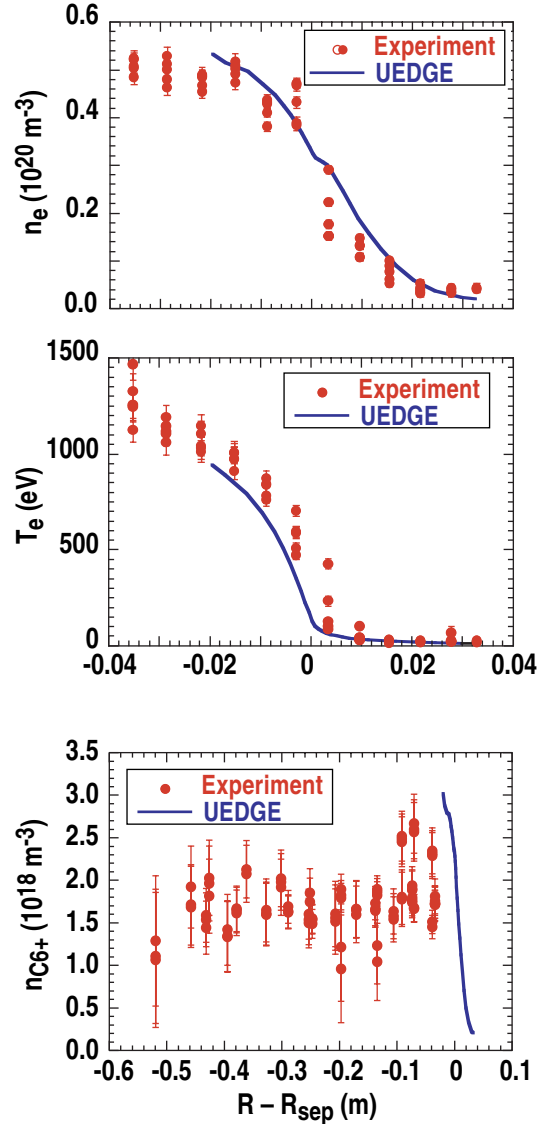


Fig. 4. Comparison of steady-state UEDGE solution with data between ELMs for midplane (a) n_e , (b) T_e and (c) $n_{\text{C6+}}$ profiles.

to the original steady-state solution within the experimental ELM period so detailed simulations with multiple ELMs will be required in the future. For the single ELM simulation at high time resolution, synthetic diagnostics were developed for UEDGE to calculate the time dependent line-integrated D_α on the DIII-D filterscope chords [Fig. 5(a,b)]. In the simulations there is an initial rapid response, within $\sim 100 \mu\text{s}$, on the outer filterscopes after the increase in D at 1.0 ms but the corresponding response on the inner filterscopes occurs several hundred microseconds later. The subsequent increase of thermal diffusivities at 1.5 ms produces nearly simultaneous responses in both divertors in the simulation but this perturbation is small compared with the response to the particle diffusivity change. The nearly simultaneous response across the outer target in the simulations is consistent with filterscope data for two chords viewing the outer divertor [1]. The time correlations of simulation chords that view the same flux surface in the inner and outer divertors [Fig. 5(c)] shows delays of the inner response of between 220 - 960 μs . The calculated correlation function for the outer most flux surface in the simulation (1.1 cm at the midplane) shows a delay of 2404 μs , similar to the $\sim 300 \mu\text{s}$ delays of Fig. 1. Finally, the simulated 2-D time evolution of CIII emission shows an increase in the outer divertor target region during the ELM consistent with the data [2]. However, it also shows the zone of CIII emission in the inner divertor leg moving away from the target during the ELM in contrast to the CIII evolution from the experiment [2] in which the CIII zone moves toward the target during the ELM.

3. Summary

Delays of the D_α response to ELMs in the inner vs. outer divertor seen both in experimental measurements [1] and initial UEDGE simulations are consistent with a simple ion convection model of ELM pulse propagation in the SOL from the outer midplane to the divertor targets. The initial UEDGE simulations show a complicated response of D_α near the divertor targets that agrees with measurements on the outer SOL flux surfaces but does not match the data near the strikepoints. The inner divertor response of CIII does not match the data but the outer leg CIII

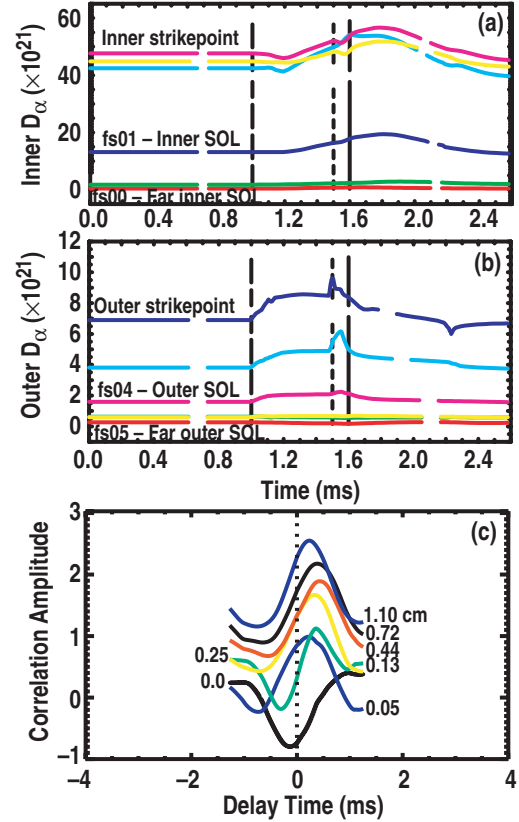


Fig. 5. Simulated filterscope signals during ELM versus time for (a) inner chords and (b) outer chords. Times shown for increase in diffusivity (dashed), increase in thermal conductivity (dotted) and ELM end (solid). Correlation of inner vs outer chords on the same flux surface shown in (c).

response is similar to the measurements. Several model refinements are indicated as a result of these initial simulations and will be pursued.

Work supported by the U.S. Department of Energy under Contract Nos. DE-AC03-99ER54463, W-7405-ENG-48, DE-FG03-95ER54294, DE-AC05-00OR22725, DE-AC02-76CH03073, DE-AC04-94AL85000, DE-FG03-01ER54615.

- [1] Fenstermacher, M.E. *et al.*, "ELM Particle and Energy Transport in the SOL and Divertor of DIII-D," accepted for publication in PPCF 2003 Special Issue on ELMs.
- [2] Groth, M *et al.*, J. Nucl. Mater., **313-316**, (2003) 1017
- [3] Boedo, J *et al.*, "ELM Dynamics and Transport in the SOL of the DIII-D Tokamak," submitted to PoP.
- [4] Takahashi, H. *et al.*, "Current in Scrape-off Layer Plasmas in DIII-D Tokamak," this conference
- [5] Loarte, A. *et al.*, Nucl. Fusion, **42**, (2002) 733
- [6] Rognlien, T.D. *et al.*, J. Nucl. Mater. **196-198**, (1992) 80.
- [7] Rognlien, T.D. *et al.*, J. Nucl. Mater., **313-316**, (2003), 1000.
- [8] Davis, J.W., Haasz, A.A., J. Nucl. Mater., **241-243** (1997) 37.